Supplemental Material

Online Figures I-VIII

Online Table I

Online Figure I

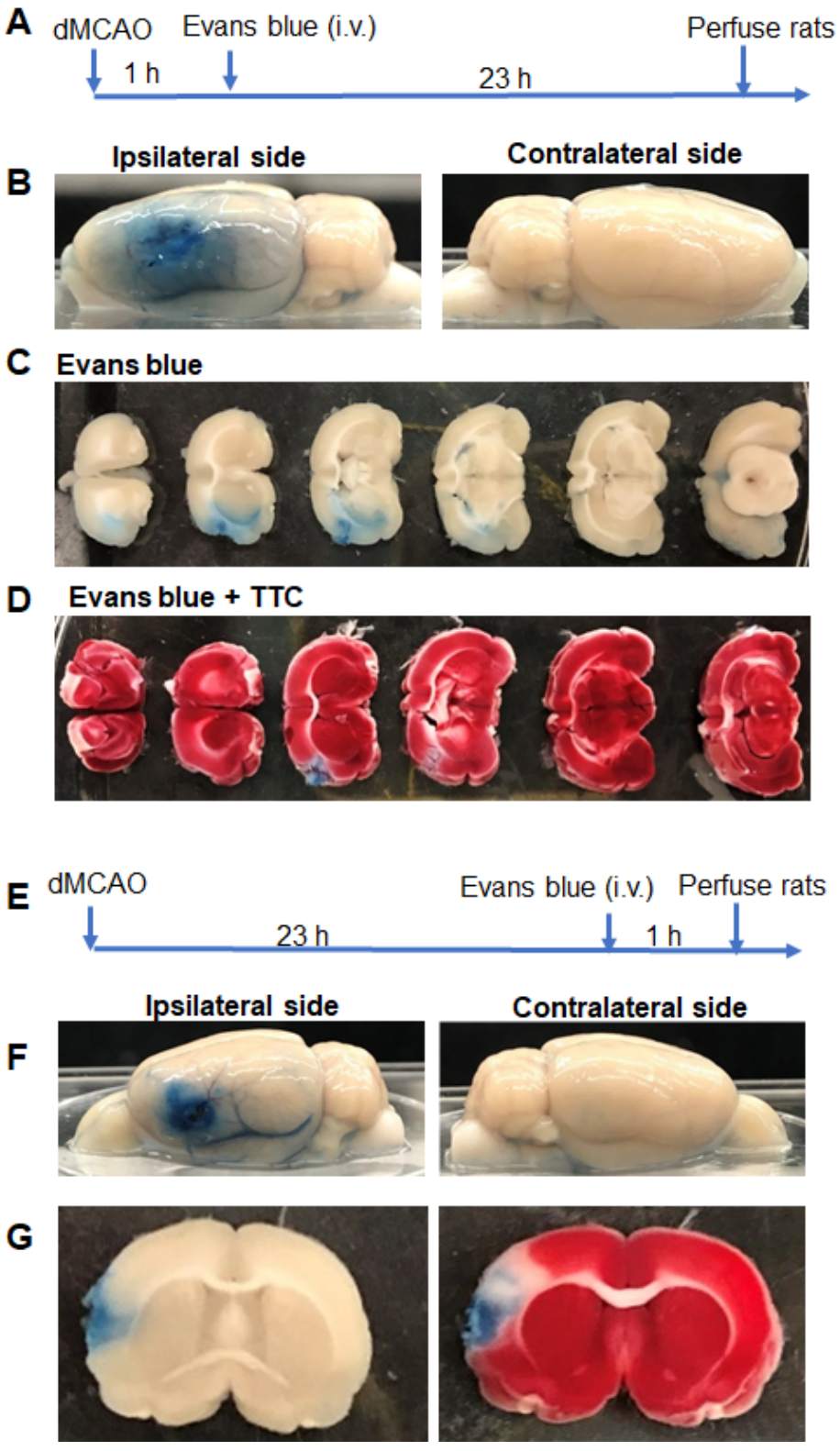

Online Figure I. Evidence for BBB leakage after ischemic stroke. A. Scheme of experimental design and workflow. A PBS-based solution containing 2% Evans Blue (EB) was intravenously injected 1 h after permanent dMCAO, and the rats were sacrificed 23 h after injection. **B.** Representative whole-mount images showing EB extravasation in the ipsilateral but not contralateral sides after dMCAO. **C.** Representative microscopic images of coronal brain sections after EB injection. EB accumulation was visible both in the ischemic core and penumbra. **D.** Representative macroscopic images of EB leakage (blue) combined with TTC staining 24 h after dMCAO. **E.** Alternative experimental timeline. A PBS-based solution containing 2% EB was intravenously injected 23 h after permanent dMCAO, and the rats were perfused 1 h after injection. **F.** Similar to (A), representative whole-mount images showing EB extravasation in the ipsilateral but not contralateral sides after dMCAO. **G.** Similar to (C-D), representative macroscopic image of EB extravasation (blue) in unstained (left panel) and TTC-staining (right panel) coronal brain sections.

Online Figure II

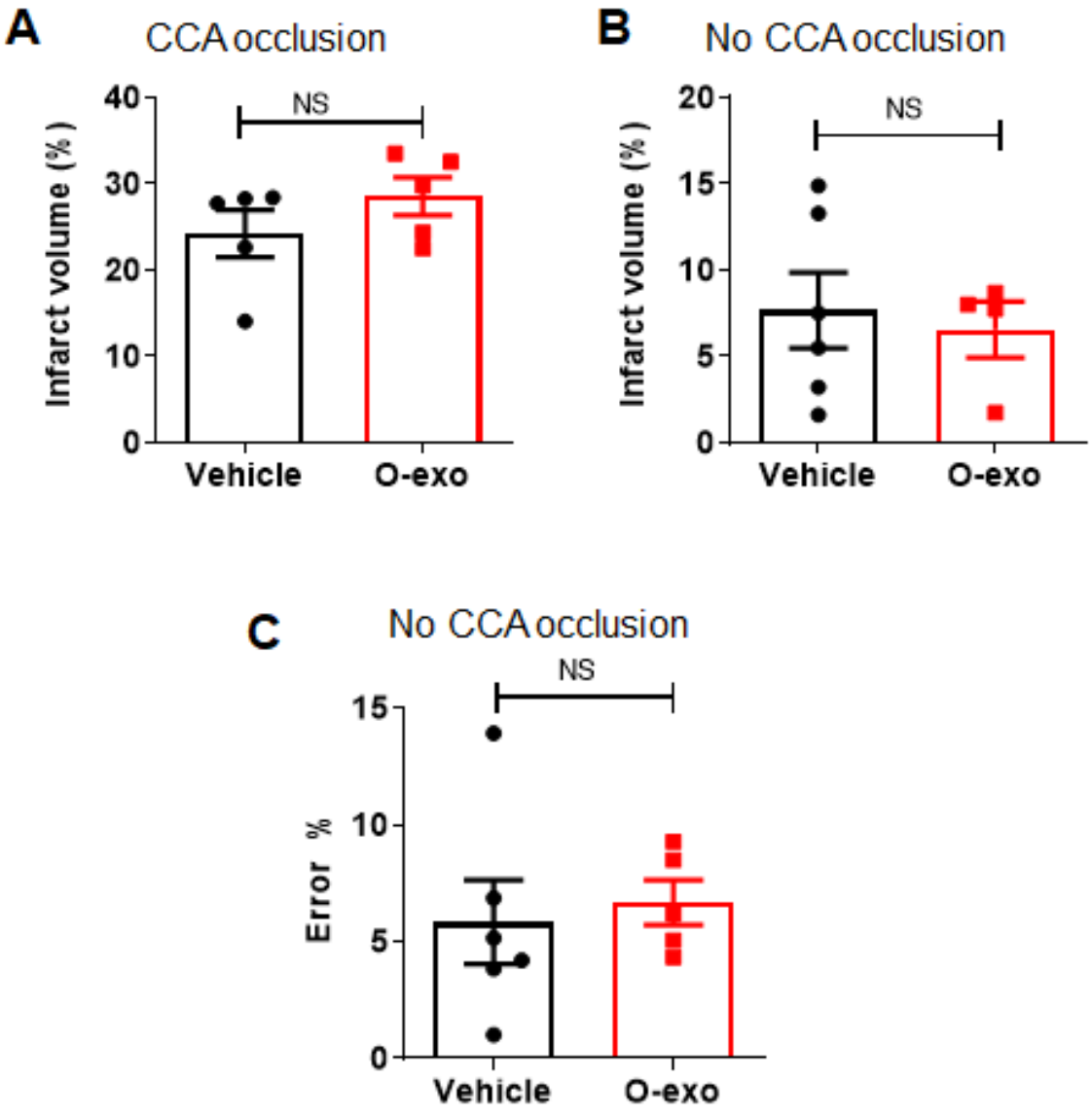

Online Figure II. Effects of O-exo on stroke outcome in young rats. A and **B.** Quantitative analysis of infarct volume in young rats treated with vehicle or O-exo 72 h after ischemic stroke with **(A)** or without **(B)** a transient bilateral CCA occlusion (N = 5 per group). The data were analyzed by a Mann-Whitney test. **C.** Young ischemic rats were treated with vehicle (N = 6 per group) or O-exo (N = 5 per group) and sensorimotor deficits were assessed by a ladder rung walking test 72 h after dMCAO. The data were analyzed by a Mann-Whitney test. NS stands for not significant. O-exo, serum exosomes from aged rats.

Online Figure III

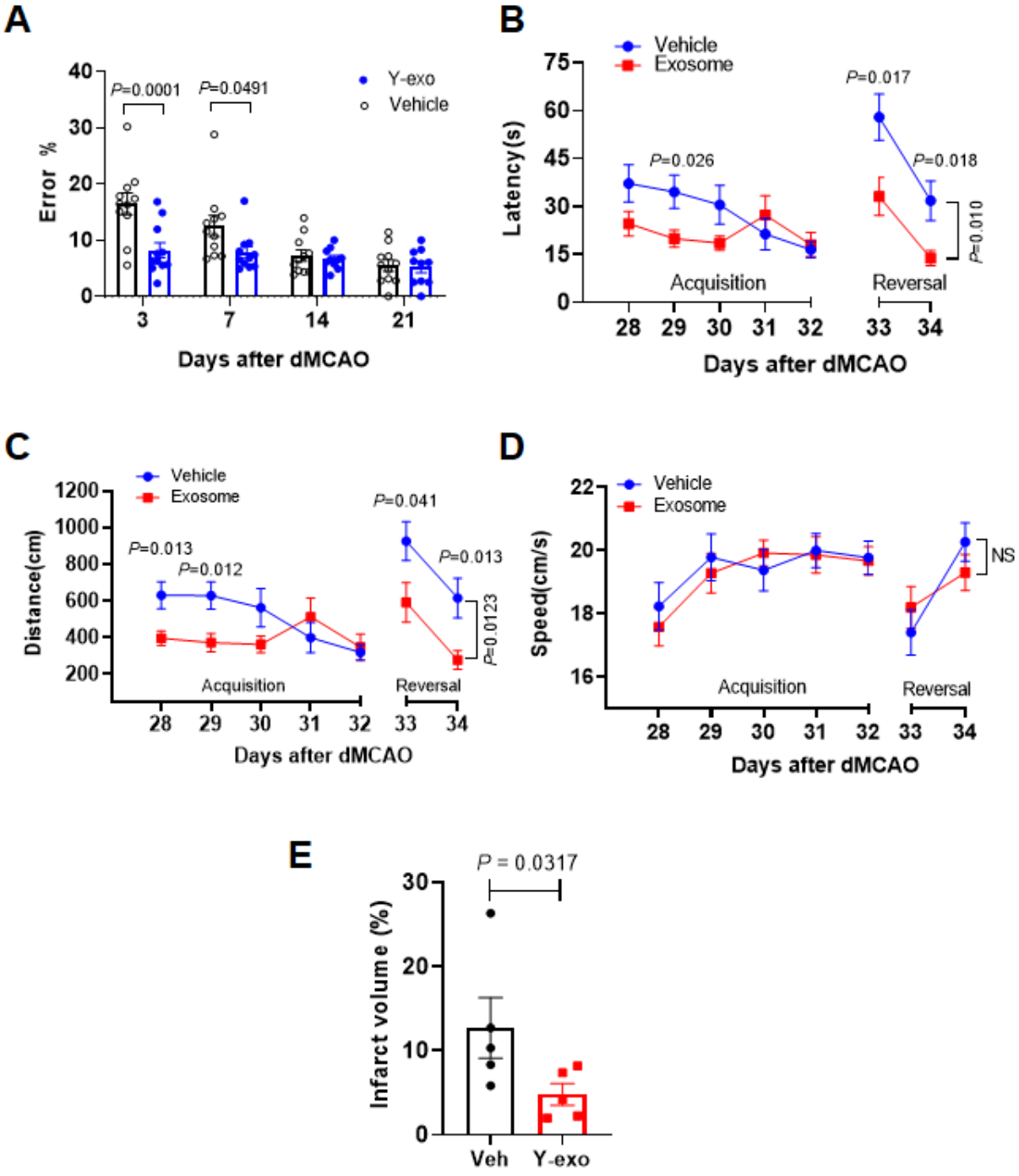

Online Figure III. Long-term effects of serum exosomes on sensorimotor and cognitive functions and infarct volume after dMCAO. A. Sensorimotor deficits in aged ischemic rats were assessed by the ladder rung walking test 3-21 days after administration of vehicle or Y-exo (N = 11 per group). The P values were assessed by a two-way repeated measures ANOVA with a post-hoc Bonferroni multiple comparisons test. **B** and **C.** MWM test was used to investigate cognitive function in aged ischemic rats 28-34 days after Y-exo or vehicle treatment. Overall, the rats treated with Y-exo exhibited significantly shorter escape latency (B) and swimming distance (C). The sample size was N = 11 per group. The P values were assessed by a two-way repeated measures ANOVA with treatment and time point as factors along with a Bonferroni multiple comparisons test. The data for the effect of treatment across the time points were analyzed by a one-way ANOVA followed by pairwise comparison using a Bonferroni as a post-hoc test. **D.** Both groups had similar swim speeds, thereby showing similar sensorimotor skills (N = 11 per group). The data were analyzed by a two-way repeated measures ANOVA test. **E.** Quantitative analysis of infarct volume using Cresyl Violet staining in vehicle– or Y-exo–treated rats 35 days after dMCAO (N = 5 per group). The P values were assessed by a Mann-Whitney test. NS stands for not significant. Y-exo, serum exosomes from young rats; O-exo, serum exosomes from aged rats. V, vehicle. Data are presented as the mean ± SEM.

Online Figure IV

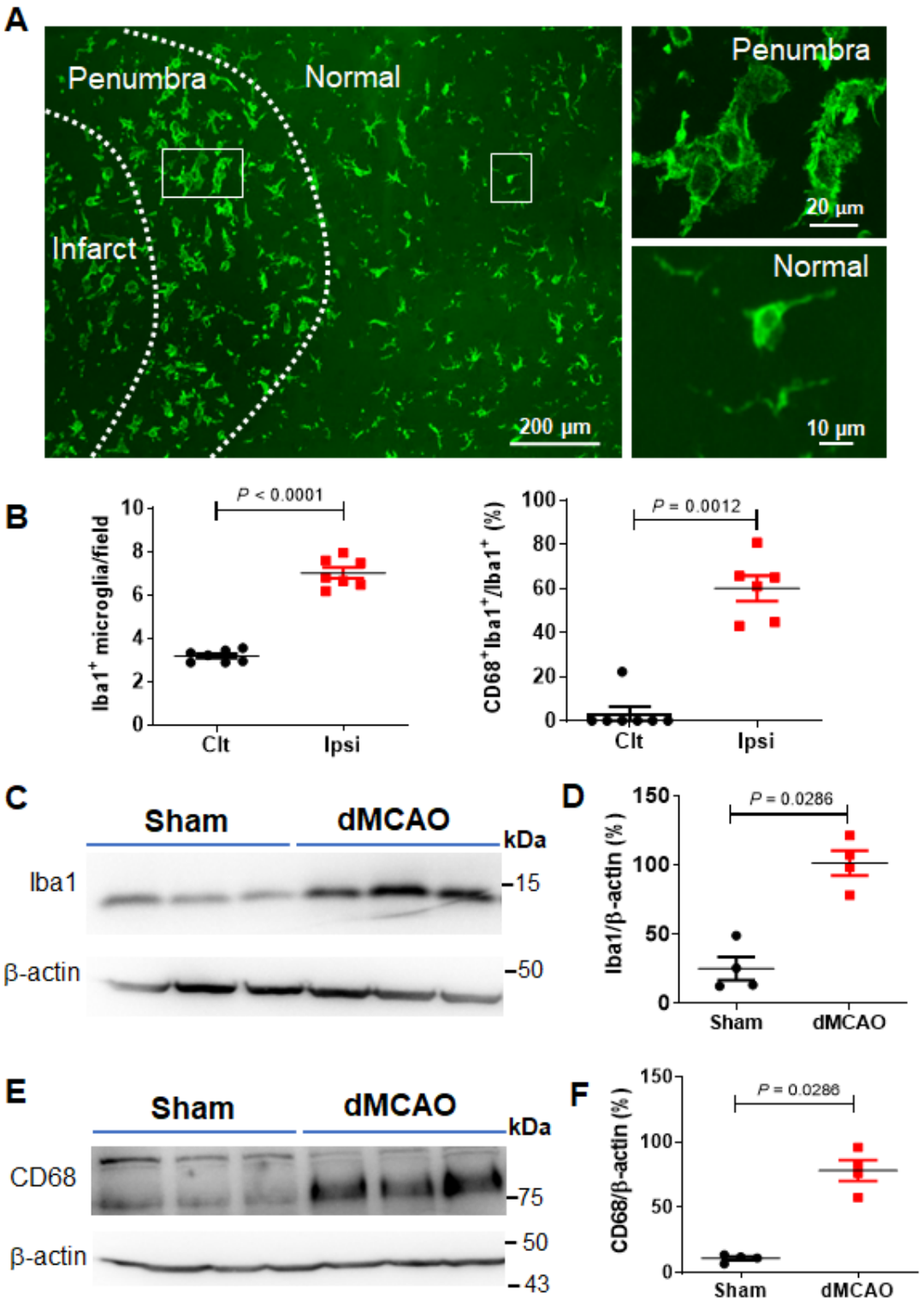

Online Figure IV. Focal ischemic stroke induces significant microglial response in the ischemic penumbra. A. Immunocytochemistry showed distribution patterns of $Iba1^+$ cells in the ipsilateral cortex suggestive of elevated microgliosis in the penumbra. Left panel: a low-magnification view of $Iba1^+$ cells in the infarct core, penumbra and adjacent healthy area. Top right panel: a typical morphology of activated microglia in the penumbra. Bottom right panel: a typical morphology of dormant microglia in the healthy area. **B.** Quantitative analysis of $Iba1^+$ microglia (left graph; N = 7 per group) and $Iba1^+CD68^+$ microglia (right panel) in the contralateral (Clt; N = 7 per group) and ipsilateral (Ipsi; N = 6 per group) cortices of aged rats 72 h after dMCAO. The P values were assessed by an unpaired Student *t*-test (left panel) and a Mann-Whitney test (right panel). **C.** Western blots show an increased expression of Iba1 protein in the ischemic cortex relative to sham. β-actin was used as a protein loading control. **D.** Relative quantification of Iba1 protein detected by Western blot in sham-operated and ipsilateral cortices after dMCAO. **E.** Western blots show an increased expression of CD68 protein in the ischemic cortex, as compared to a sham-operated control. β-actin was used as a protein loading control. **F.** The expression levels of CD68 protein detected by Western blot in sham-operated and ipsilateral cortices after dMCAO were normalized to the β-actin level. Data are presented as the mean ± SEM. Each data point represents a biological replicate. The P values in D and F were assessed by a Mann-Whitney test. Clt, contralateral; Ipsi, ipsilateral.

Online Figure V

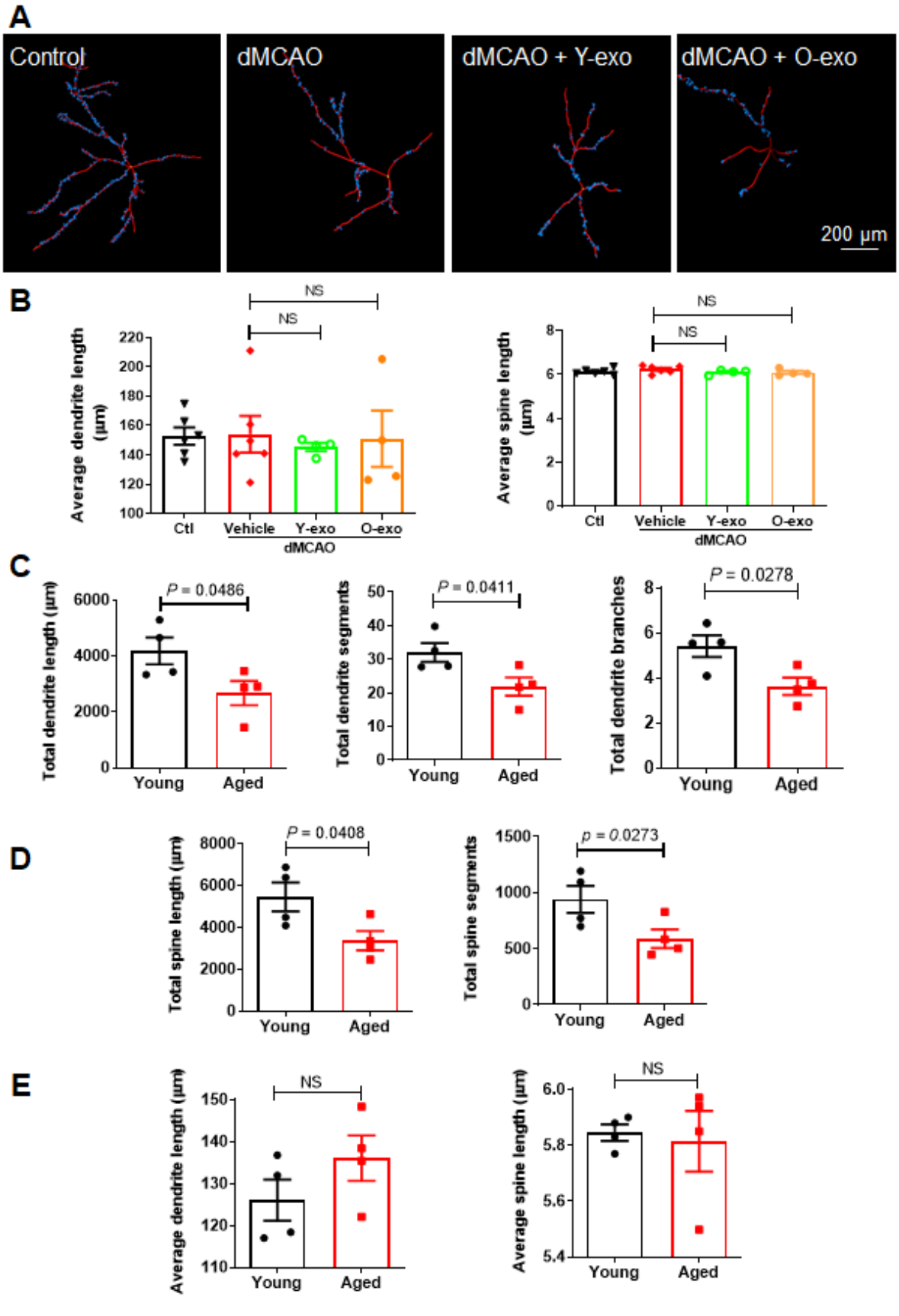

Online Figure V. Effects of serum exosomes and aging on the number of dendrites and spines. A. A representative three-dimensional reconstruction of a Golgi-Cox–stained pyramidal neuron and a semi-automated trace generated by Filament Tracer using Imaris software in each group as indicated. **B.** Quantitative analyses of the effects of vehicle or serum exosomes on the average dendritic (left panel) and average spine (right panel) length in the penumbra and the corresponding contralateral cortical areas (Ctl) 72 h after vehicle, Y-exo or O-exo treatments. Each data point represents a biological replicate. The data were analyzed by a Kruskal-Wallis test with a Dunn's post-hoc multiple comparison test. **C** and **E.** Quantitative analyses of the total dendritic length (left graph), the total dendritic segments (middle graph) and the total dendritic branches (right graph) **(C)**, total spine length (left panel) and total spine segments (right panel) **(D)**, and average dendritic length (left panel) and average spine length (right panel) **(E)**. Each data point represents a biological replicate. The P values were assessed by an unpaired Student *t*-test (C and D) and a Mann-Whitney test (E). The data were acquired from cortical layers II/III and V pyramidal neurons obtained from young and aged rats and viewed at 60× magnification. NS stands for not significant. Y-exo, serum exosomes from young rats; O-exo, serum exosomes from aged rats.

Online Figure VI

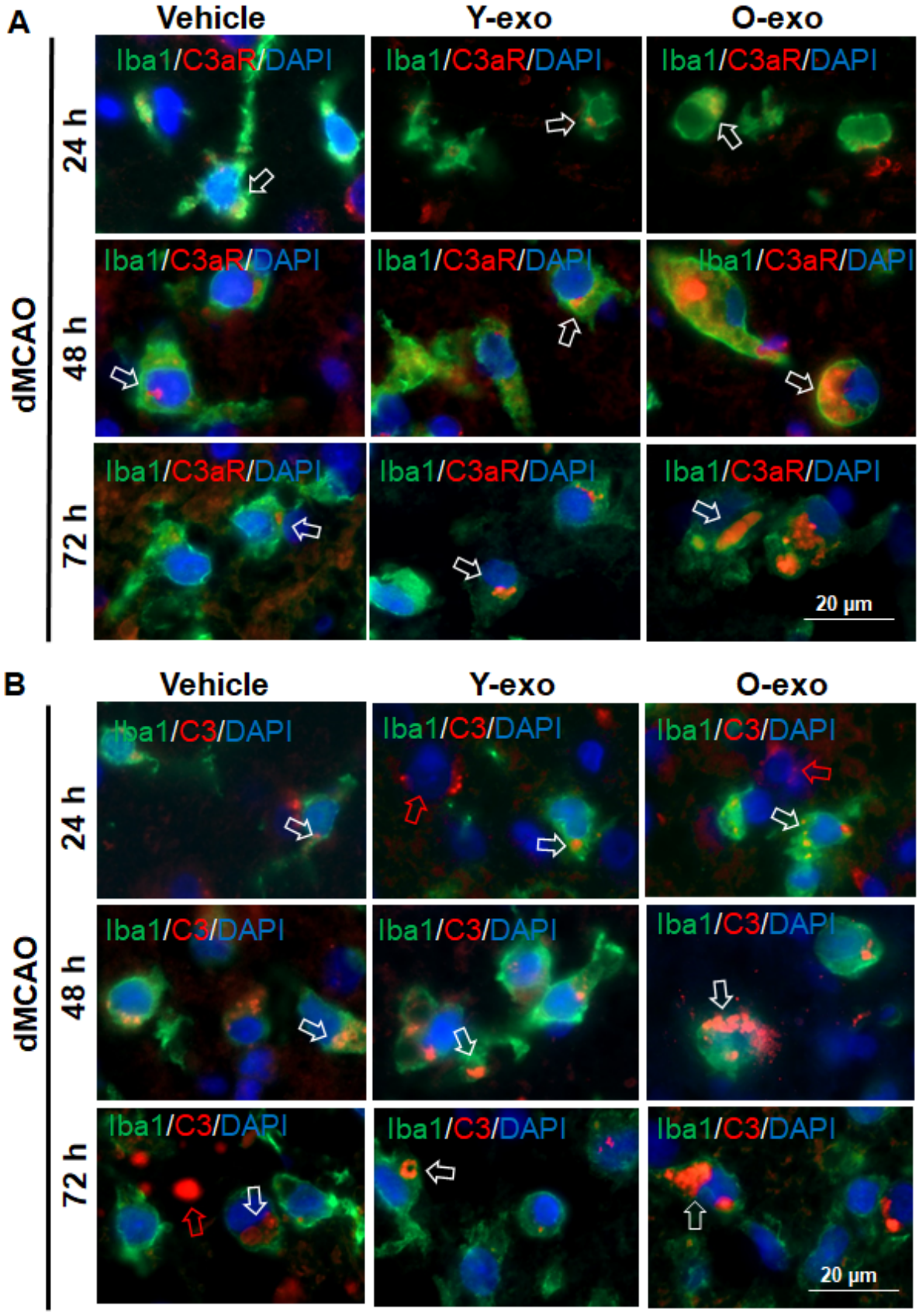

Online Figure VI. The time course and expression levels of microglial C3aR and C3 (C3a/b) in aged ischemic rats after injection of Y-exo or O-exo. A. Representative microscopic images of double immunostaining shows that C3aR (red) is expressed in $Iba1^+$ (gree) microglia on the ischemic penumbra 24, 48 and 72 h after injection of Y-exo, O-exo or vehicle. The expression level of microglial C3aR is noticeably increased 48 and 72 h in aged ischemic rats injected with O-exo. DAPI (blue) was used as a nuclear counterstain. **B.** Representative microscopic images of double immunostaining for C3 (C3a/b) (red) and $Iba1^+$ (green) show the expression levels of C3a/b in $Iba1^+$-labeled microglia in the ischemic penumbra 24, 48 and 72 h after injection of Y-exo, O-exo or vehicle. Arrows indicate specific sites of co-labeling in microglia. Red arrows indicate non-microglial cells. DAPI (blue) was used as a nuclear counterstain. Y-exo, serum exosomes from young rats; O-exo, serum exosomes from aged rats.

Online Figure VII

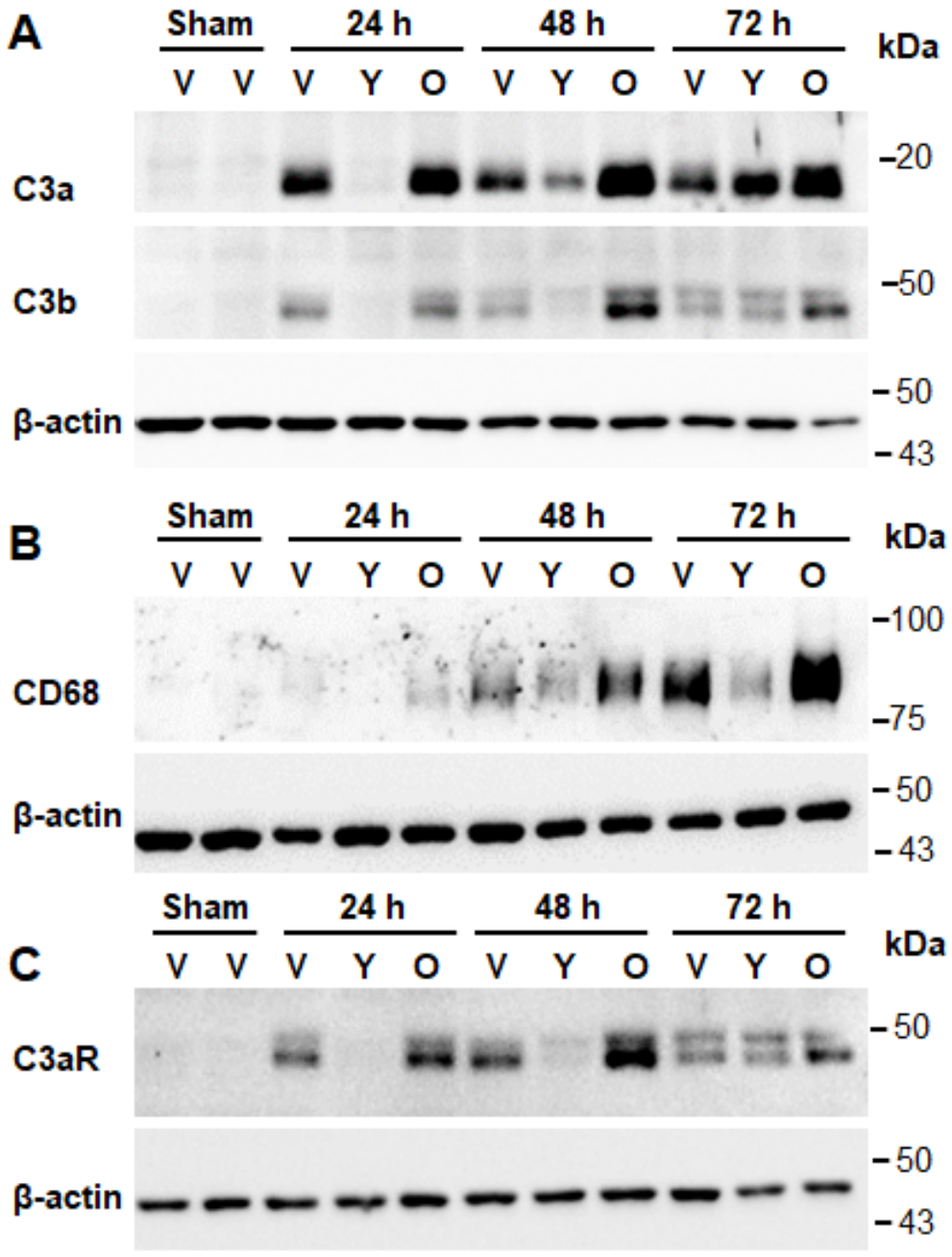

Online Figure VII. Expression levels of C3a, C3b, CD68 and C3aR in the ipsilateral cortex of aged ischemic brain 24, 48 and 72 h after injection of Y-exo or O-exo. A to **C.** Vehicle, Y-exo or O-exo were intravenously injected into aged ischemic rats. The proteins were isolated from ipsilateral cortex 24, 48 and 72 after ischemic stroke. The cerebral cortex from sham-operated rats (Sham) was used as a control. Western blots were performed using antibodies as indicated. β-actin was used for a protein loading control. Y, serum exosomes from young rats; O, serum exosomes from aged rats; V, vehicle.

Online Figure VIII

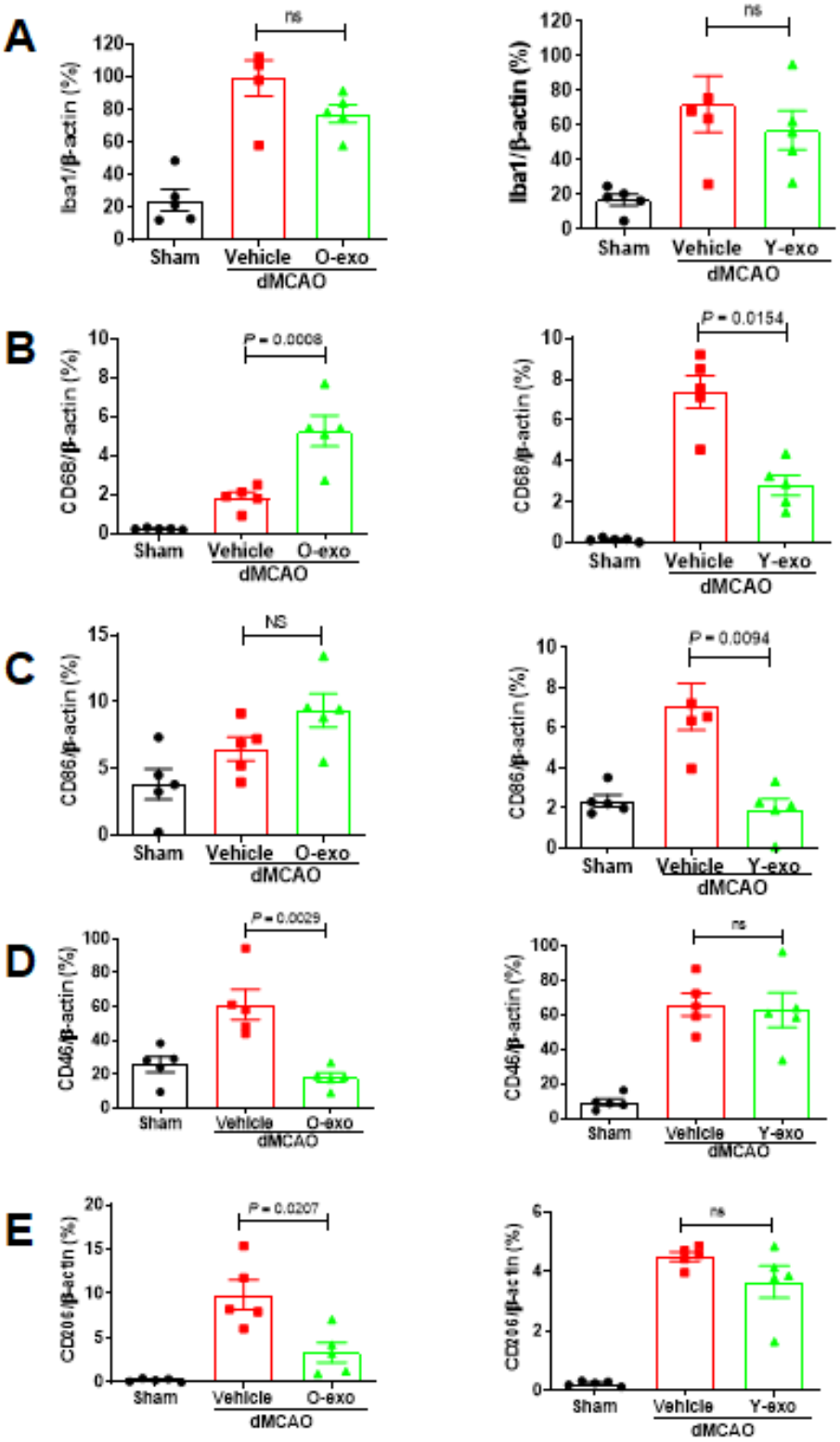

Online Figure VIII. Expression levels of microglial proteins in healthy and ipsilateral cortices of aged rat brain after injection of Y-exo or O-exo. A to **E.** Vehicle, Y-exo or O-exo were intravenously injected into aged ischemic or aged sham-operated rats. The proteins were isolated from healthy (aged sham-operated rats) or ipsilateral (aged ischemic rats) cortices 72 h after dMCAO. Western blots were performed using antibodies against microglial protein markers. β-actin was used to a protein loading control. The expression levels of Iba1 **(A)**, CD68 **(B)**, CD86 **(C)**, CD46 **(D)** and CD206 **(E)** were normalized to the β-actin level and determined using the ChemiDoc Imaging System. Data are presented as the mean ± SEM. Each data point represents a biological replicate. The P values were assessed by a Kruskal-Wallis test with a Dunn's *post-hoc* multiple comparison test. Y-exo, serum exosomes from young rats; O-exo, serum exosomes from aged rats.

Online Table I. Change in plasma cytokine levels in normal and ischemic aged rats treated with vehicle, young and old serum exosomes (N=4 per group).

Cytokines	Normal (AVG ± SE)	Vehicle (AVG ± SE)	Y-exo (AVG ± SE)	O-exo (AVG ± SE)
G-CSF	15.4 ± 4.4	3.8 ± 3.8	7.7 ± 7.7	5.1 ± 3.3
Eotaxin	13.9 ± 0.6	13.6 ± 1.0	13.8 ±0.7	13.6 ± 2.6
GM-CSF	0.0 ± 0	0.0 ± 0	0.0 ± 0	0.0 ± 0
IL-1a	82.2 ± 12.5	68.8 ± 15.9	87.8 ± 5.1	106.9 ± 27.8
Leptin	24131.5 ± 2484	19274.9 ± 2166	24752.1 ± 1683	14058.1 ± 3516
MIP-1a	16.3 ± 1.4	25.2 ± 5.2	21.0 ± 1.3	22.3 ± 3.0
IL-4	42.9 ± 12.7	60.3 ± 17.6	56.2 ± 10.8	78.1 ± 16.0
IL-1B	42.1 ± 6.3	53.1 ± 22.0	55.1 ± 10.2	46.1 ± 4.2
IL-2	162.6 ± 18.5	159.2 ± 62.4	171.0 ± 9.6	202.3 ± 58
IL-6	1713.5 ± 160.0	1365.4 ± 276.3	1748.7 ± 219.2	1996.1 ± 501.5
EGF	0.0 ± 0	0.5 ± 0.5	0.2 ± 0.1	1.0 ± 0.9
IL-13	36.4 ± 3.6	25.9 ± 6.1	37.5 ± 4.2	29.7 ± 3.9
IL-10	62.9 ± 5.0	58.9 ± 20.7	54.2 ± 5.0	45.6 ± 8.9
IL-12	186.5 ± 26.6	238.1 ± 74.9	254.1 ± 12.2	264.6 ± 57.2
IFNy	112.4 ± 18.5	135.1 ± 34.0	147.9 ± 41.0	187.2 ± 54.4
IL-5	90.8 ± 5.0	93.7 ± 13.0	93.1 ± 4.0	98.1 ± 17.2
IL-17A	33.8 ± 1.0	46.3 ± 9.8	49.6 ± 4.0	51.2 ± 10.4
IL-18	214.4 ± 25.4	280.1 ± 40.2	251.7 ± 30.7	302.4 ± 66.4
MCP-1	1181.1 ± 220.1	1614.1 ± 432.5	1610.1 ± 47.0	1375.1 ± 132.8
IP-10	393.9 ± 381.2	381.2 ± 10.8	365.4 ± 28.1	353.8 ± 70.7
VEGF	37.0 ± 2.3	58.6 ± 13.0	53.3 ± 2.5	64.7 ± 14.0
Fractalkine	35.4 ± 1.4	49.9 ± 7.0	53.0 ± 1.6	52.8 ± 7.7
LIX	1089.8 ± 94.0	1396.0 ± 219.0	1055.0 ± 79.0	1050.9 ± 95.4
TNFa	9.9 ± 1.5	10.6 ± 4.4	13.8 ± 1.9	15.9 ± 2.7
RANTES	2247.6 ± 57.6	2810.7 ± 425.6	2338.1 ± 247	2350.6 ± 288.5
GM-CSF	0.0 ± 0	0.0 ± 0	0.0 ± 0	0.0 ± 0
GRO/KC	0.0 ± 0	0.0 ± 0	0.0 ± 0	0.0 ± 0
MIP-2	0.0 ± 0	0.0 ± 0	0.0 ± 0	0.0 ± 0

The concentrations of cytokines/chemokines in the samples and expressed as pg/mL.